

Electron scattering on molecules: search for semi-empirical indications^{*}

Kamil Fedus^a and Grzegorz P. Karwasz

Institute of Physics, Faculty of Physics, Astronomy and Informatics, Nicolaus Copernicus University, Grudziadzka 5/7, 87-100 Toruń, Poland

Received 30 January 2017 / Received in final form 9 April 2017

Published online 6 June 2017

© The Author(s) 2017. This article is published with open access at Springerlink.com

Abstract. Reliable cross-sections for electron-molecule collisions are urgently needed for numerical modeling of various processes important from technological point of view. Unfortunately, a significant progress in theory and experiment over the last decade is not usually accompanied by the convergence of cross-sections measured at different laboratories and calculated with different methods. Moreover the most advanced contemporary theories involve such large basis sets and complicated equations that they are not easily applied to each specific molecule for which data are needed. For these reasons the search for semi-empirical indications in angular and energy dependencies of scattering cross-section becomes important. In this paper we make a brief review of the applicability of the Born-dipole approximation for elastic, rotational, vibrational and ionization processes that can occur during electron-molecule collisions. We take into account the most recent experimental findings as the reference points.

1 Introduction

Cross sections for electron scattering on atoms and molecules are the input data for modeling plasmas in thermonuclear reactors [1,2], interstellar media [3] and plasma etching [4]. Extensive sets of cross sections in a wide energy range, from few ten of eV to thousand eV, are needed also for predicting radiation damage in biological tissues [5]. Required data comprise the total cross sections which measure the overall scattering probability and the partial cross sections, i.e. probabilities of separate channels such as production of specific ions.

Knowledge of every different processes is essential in specific fields. In radiation damage these are ionization processes (total ionization cross section that gives information on the amount of low-energy electrons produced) and dissociative attachment processes at near-to-zero energy (decisive for the DNA cutting [5]). In plasma etching, instead, partial ionization and dissociation into radical cross sections (and channels via which they undergo) are essential. For tokamak plasma diagnostics these are electronic excitation and optical emission cross sections, while for energy transport and cooling – vibrational and rotational cross sections are needed.

Total cross sections are the easiest to be measured in absolute way via attenuation method. But only in some

gases, for example CH₄, agreement between different measurements is good, so recommended values with as little as 5% uncertainty can be drawn [6]. For polar molecules such as H₂O and NH₃ serious disagreements, up to few folds, exists between different experiments at low energies. This is due to the forward-centered scattering on a long-range dipole potential, so the angular resolution error (see for example Ref. [7]) underestimates measured total cross section. The difficulty stays in the evaluation of the small-angle contribution to this scattering.

Vibrational excitation, in particular via resonant processes is an important channel of thermonuclear plasma cooling at few eV energy range. However, as we showed for CH₄ [6,8] a rather serious disagreement exists between different theories and experiments. Some independent evaluations are still needed.

In this paper we study briefly the applicability of the Born-dipole approximation (also known as the first Born approximation) to elastic, rotational, vibrational and ionization scattering channels for electron collisions with polar molecules taking into account the most recent experimental findings. This approximation refers to weak scattering (i.e. a feeble interaction between electron and target) and it is generally assumed to be valid at high incident energies (applicable for electronic excitation, dissociation, ionization) or at energy thresholds of inelastic processes (rotational and vibrational excitations) where the electron-molecule collisions are dominated by long-range forces [9,10]. In addition a low energy-low angle elastic interaction with strongly polar targets is also considered

^{*} Contribution to the Topical Issue “Atomic and Molecular Data and Their Applications”, edited by Gordon W.F. Drake, Jung-Sik Yoon, Daiji Kato, and Grzegorz Karwasz.

^a e-mail: kamil@fizyka.umk.pl

as the domain of Born approximation. Since the time of its formulation [9,10] the Born-dipole models have been derived for different processes and compared with experiments and theories. Sometimes this approximation was found to be enough good and sometimes was judged as completely wrong. Moreover in some cases it gives better agreement with experiments than more advanced (less approximative) calculations. So far, except general conditions, little is known about the specific factors deciding on the validity of this approximation for particular targets and scattering channels because no systematic studies on this issue have been carried out and the literature data are very scattered. Only recently, Tanaka et al. [11] made a compact review of scaled plane-wave Born models used for a description of optically allowed electronic-state excitations.

Since the uncertainty estimates in theoretical calculations is currently an important issue [12], particularly for plasma modelling purposes, here we give the Born cross-sections with error bars assuming some uncertainties on the fundamental molecular quantities involved in the Born formulas for different partial processes. The goal is to show how the changes in some molecular parameters affect the tested models.

2 Elastic scattering

The angular dependence of elastic differential cross-sections (DCS^{el}) for majority of polar molecules can be clearly divided into two parts: (i) a high-angle scattering (typically higher than 10°), which is governed by the short-range forces and (ii) the low-angle scattering (typically lower than 10°) driven by the long-range effects due to electron-permanent dipole interaction. The competition between both types of interaction is energy-dependent with the importance of long-range forces extending over wider angular range with decreasing electron energy. Consequently, low-energy DCS are strongly forward-centered. From theoretical point of view, the presence of the dipolar interaction is troublesome since the forward scattering amplitude is diverging for any electron energy in the fixed-nuclei approximation and rotations has to be taken into account to make this quantity finite. The recent review paper by Fabrikant [13] describes in details advances in theoretical approaches undertaking this problem.

Experimentally it is also difficult to characterize DCS for polar molecules, particularly at low scattering angles, due to the finite acceptance angle of detectors. Nevertheless the most recent experimental studies using improved experimental systems show that low-angle and low-energy elastic DCSs can be well described in the first Born approximation (considering the incoming electron wave function to be weakly perturbed by the target molecule what is true when the scattering occurs at large distances) and treating the molecule as the fixed point-dipole. Under such approximations Altshuler [14] derived a simple formula for elastic DCS (in atomic units):

$$DCS^{el} = \frac{2D^2}{3k^2}(1 - \cos\theta)^{-1}, \quad (1)$$

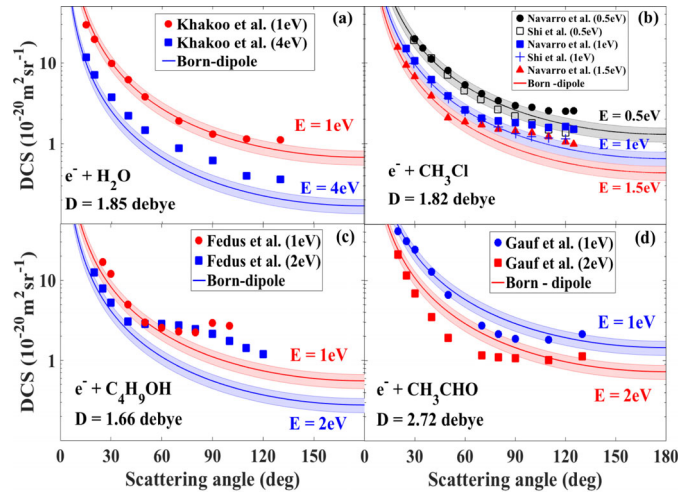


Fig. 1. Elastic differential cross-sections versus the scattering angle at low energies for (a) water vapour, H_2O , (b) chloromethane, CH_3Cl , (c) isobutanol, C_4H_9OH , and (d) acetaldehyde, CH_3CHO : the comparison between experimental data and the Born-dipole model (Eq. (1)). Experiments: Khakoo et al. [15,16], Navarro et al. [19], Shi et al. [20], Fedus et al. [21] and Gauf et al. [22]. The shaded areas represent the error bars for the Born cross-sections when 10% uncertainties are assumed on the molecular dipole moments.

where k is the incident electron momentum, D is the permanent dipole moment of the molecule and θ is the scattering angle. As mentioned above, since no rotations are included, the DCS diverges at $\theta = 0^\circ$, but it is well behaved for $\theta \neq 0^\circ$. For example, Khakoo et al. [15,16] noticed a very good agreement in shape and magnitude between the measured values of low-angle DCSs of H_2O and the pure Born-dipole approximation ($D = 1.85$ D [17,18]) below $E = 4$ eV (see Fig. 1a). Note that at 1 eV equation (1) remains consistent with experimental data up to 130° ! The similar situation, but less pronounced, is observed for other polar molecules which were characterized at 1 eV or lower energies: chloromethane (CH_3Cl , $D = 1.89$ D [18]), isobutanol (C_4H_9OH , $D = 1.66$ D [18]) and acetaldehyde (CH_3CHO , $D = 2.71$ D [18]) as shown in Figures 1b–1d. The common feature for all these targets is the fact that with increasing energy the forward peak of DCS is confined in narrower angular range [19–22]. This behavior reflects the increasing influence of the short-range interactions, as the energy increases.

It is necessary to mention that all experimental data points shown in Figure 1 contain the contribution of both elastic and rotationally inelastic scattering because the experiments are not able to distinguish between the two. Crawford [23] using the model of rotating rigid dipole (see equations in Sect. 3) showed that in the limit of high moments of inertia (i.e. for very small momentum transfer between electron and molecule) the cross-sections summed over all final rotational states and averaged over all populated initial states are reduced to the relations derived in the stationary point-dipole approximation. Hence equation (1) should be valid when molecules have very small

energy level spacing between rotational states with respect to the energy of incident electron. The validity conditions for this approximation are still to be determined for the specific targets.

The integration of equation (1) over the entire angular range allows to derive a formula for a momentum transfer cross-sections (MTCS): $\sigma_{mt}^{el} = \int_0^\pi DCS \cdot (1 - \cos \theta) \sin \theta d\theta$, the quantity important in modeling of transport phenomena in plasmas and gases [14]:

$$\sigma_{mt}^{el} = \frac{8\pi D^2}{3k^2}. \quad (2)$$

Crawford [23] showed that exactly the same expression can be derived for MTCS (summed over all final states and averaged over initial rotational states) within the model of rotating rigid dipole in the limit of high moments of inertia. Moreover he stated that at “sufficiently” low energies this expression could be a very good approximation to exact solutions of the model for any polar molecule regardless of its size, shape and symmetry. Similar conclusion was reached by Christophorou et al. [4,24] who suggested that equation (2) could be used as a first estimate of MTCS at near thermal energies in the absence of accurate direct measurements. In Figure 2 this equation is plotted against swarm-derived MTCS for H_2O , NH_3 ($D = 1.47$ D [18]) and CHF_3 ($D = 1.65$ D [18]). The agreement between Born-dipole approach and swarm-derived data has to be judged as good below 1 eV. Note however that MTCS shown in Figure 2 are not free of errors since they are derived through a complicated numerical analysis of Boltzmann transport equation using the experimentally determined electron transport coefficients as the input data. Moreover the numerical determination of MTCS is not unique in swarm analysis since different cross-sectional datasets can be constructed to reproduce the same set of experimentally measured coefficients, see discussion by Nakamura [25]. Ambiguity of such determination is clearly visible for H_2O , where completely different MTCSs were proposed by different authors, see reference [26] for more details. Here we show that for the latter molecule the Born-dipole approach agrees with swarm-derived cross-sections provided by Hayashi [27] and Pack et al. [28]. It is an interesting result since the full representation of Hayashi’s cross section [27] for all partial processes does not include explicitly rotational cross sections. Rotations are expected to be very important for H_2O since their contribution to total scattering was estimated to be 75% at 200 meV, see reference [29] and references therein. In other words, the Hayashi’s MTCS describes rather an “effective” (rotationally summed) momentum transfer than pure elastic one. On the other hand Yousfi and Benabdessadok [26] proposed the representation of cross sections for H_2O that includes explicitly the rotational excitation (the latter calculated within the Born approximation). Consequently, his pure elastic MTCS (see Fig. 2a) are much lower than Hayashi’s dataset and it does not follow the Born-dipole model, since the latter describes a rotationally summed elastic scattering.

The similar description should be also valid for NH_3 , but this time the “effective” and pure elastic MTCSs

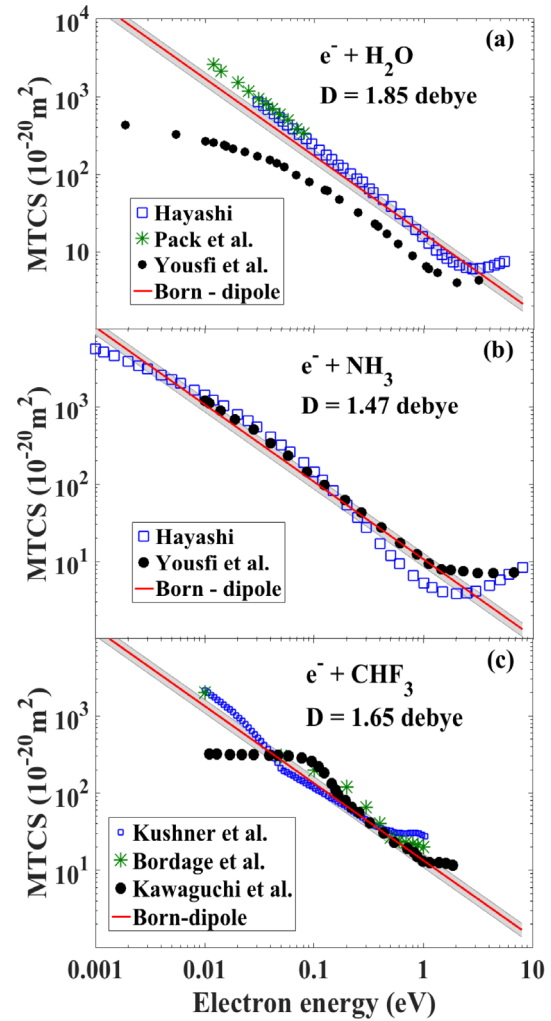


Fig. 2. Momentum transfer cross-section versus electron energy for (a) water vapour, H_2O , (b) ammonia, NH_3 , and (c) fluoroform, CHF_3 for $E < 1$ eV: the comparison between swarm-derived data and the Born-dipole model (Eq. (2)). Experiments: Hayashi [27], Pack et al. [28], Yousfi and Benabdessadok [26], Kushner and Zhang [30], Bordage and Segur [31] and Kawaguchi et al. [32]. The shaded areas represent the error bars for the Born cross-sections when 10% uncertainties are assumed on the molecular dipole moments.

by Hayashi [27] and Yousfi and Benabdessadok [26], respectively, are in relatively good agreement (see Fig. 2b). This could be explained by much lower contribution of rotational excitations derived by Yousfi and Benabdessadok [26] to the overall scattering when compared to pure elastic effect in considered energy range. This follows the same line as result obtained by Jones et al. [29] who estimated the contribution of rotational scattering to total cross-sections (TCS) of NH_3 to be roughly constant at 45% between 500 and 30 meV, hence lower than for H_2O .

For CHF_3 all three considered datasets in Figure 2c, Kushner and Zhang [30], Bordage and Segur [31] and Kawaguchi et al. [32], represent an “effective” MTCS (no rotations in full representation of CS) explaining

a relatively good agreement with the Born-dipole model. It is clear that more extensive comparative study is necessary to validate equation (2). In particular the data from electron beam experiments at low (thermal) energies would be valuable.

Unfortunately, the similar closure formula to equation (2) cannot be derived analytically for integral cross-section of elastic (or rotationally summed elastic) process since the latter quantity is divergent in the Born approximation: $\int_0^\pi DCS \cdot \sin \theta d\theta = \infty$.

3 Rotational excitations

It is generally assumed that rotational excitations play an important role in low-energy electron interaction with polar molecules. Unfortunately, the excitation energies associated to rotational levels are so low and the angular distribution of scattered electrons is so peaked in the forward direction that experiments do not have enough energy and angular resolution to distinguish elastic and rotational processes. Consequently, experimental measurements of pure rotational CS for polar molecules are extremely scarce, see review on rotational excitations by Itikawa and Mason [33]. In the low energy region the rotational CS can be estimated in Born approximation treating the molecule as the rigid rotating dipole. In this case the differential and integral cross-sections are given by the following formulas (in atomic units) [23,34,35]:

$$DCS^{rot}(j \rightarrow j') = \frac{4D^2}{3} \gamma \frac{k'}{k} \frac{1}{q^2} \delta_{j,j\pm1} \quad (3)$$

$$\sigma_{ICS}^{rot}(j \rightarrow j') = \frac{8\pi D^2}{3k^2} \gamma \log \frac{k+k'}{|k-k'|} \delta_{j,j\pm1} \quad (4)$$

$$\sigma_{mt}^{rot}(j \rightarrow j') = \frac{8\pi D^2}{3k^2} \gamma \left(1 - \frac{(k-k')}{2kk'} \log \frac{k+k'}{|k-k'|} \right) \delta_{j,j\pm1} \quad (5)$$

where k and k' are the incident and scattered electron momenta and $q^2 = k^2 + k'^2 - 2kk' \cos \theta$ is the momentum transfer squared. Here $\gamma = (j_{>}) (2j+1)^{-1}$ is for linear molecules (e.g. all diatomic, HCN, OCS) or $\gamma = (j_{>} - K^2) [(2j+1) j_{>}]^{-1} \delta_{K,K'}$ is for symmetric top molecules (e.g. NH₃, CH₃Cl) with $j_{>}$ denoting the larger of initial and final j values. Quantum number K represents the projection of total angular momentum on the molecular symmetry axis, $K = -j, -j+1, \dots, j$, for symmetric top molecules. Note that for the latter group the dipole interaction is insensitive to the rotation around symmetry axis ($\Delta K \neq 0$). In the limit of high moment of inertia equations (3) and (5) are reduced to equations (1) and (2), respectively, while σ_{ICS}^{rot} becomes divergent. Itikawa [36] derived also general formulas for asymmetric-top molecules (e.g. H₂O) in the Born approximation. In particular case of pure dipole interaction for $0_{00} \rightarrow 1_{11}$ transition the expressions of Itikawa [36] are reduced to same equations as for linear molecules.

In the first approach, all these relations can be used to quickly predict pure rotational CS at low energies. In

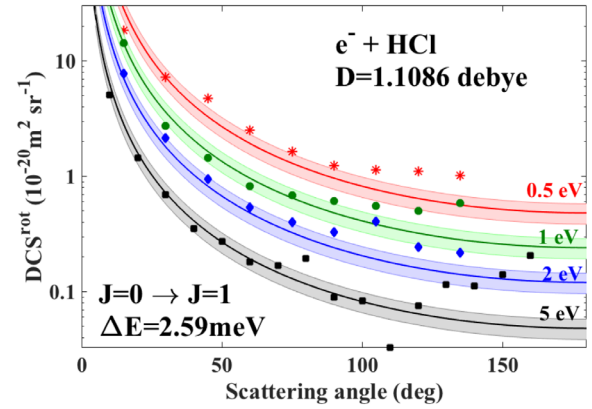


Fig. 3. Differential cross-sections for electron impact excitation of $J = 0 \rightarrow J = 1$ rotational transition in hydrochloric acid, HCl ($D = 1.1086$ D [18]). The Born-dipole model is compared with beam experimental data of Rädle et al. [37] for electron energies 0.5 eV, 1 eV and 2 eV and Gote and Ehrhardt [38] for 5 eV. The shaded areas represent the error bars for the Born cross-sections when 10% uncertainties are assumed on the molecular dipole moments.

Figure 3 we show the comparison of Born-dipole model (Eq. (3)) with experimental DCS [37,38] for $J = 0 \rightarrow J = 1$ transition in HCl measured in crossed-beam experiments at energies below 5 eV. The energy loss of $\Delta E = 2.59$ meV [33] and the dipole moment $D = 1.1086$ D [18] was used in equation (3). Moreover the uncertainty of 10% was assumed on D and the corresponding error bars are given by the shaded areas. Note that errors could be even larger if the uncertainties in energy threshold determination would be taken into account. Nevertheless these uncertainties do not affect a good agreement between the Born model and experiments. This is an encouraging result, in particular if we take into account the fact that the experimental data were obtained through a complicated numerical analysis of the broadening effect of elastic peak in electron energy loss spectrum.

So the Born dipole model has a potential to describe low-energy rotational cross-sections for some particular polar targets. Nevertheless, more extensive study is necessary since advanced calculations by Faure et al. [39] and Curik et al. [40] (both for H₂O) show that the Born-dipole approximation overestimates integral CS, though it preserves quite well the shape of energy dependence.

4 Vibrational excitations

Born approximation was proposed already in 60s and 70s for non-resonant (direct) vibrational excitation near thresholds. The differential and integral cross-sections of the vibrational transition from initial to final modes $\nu \rightarrow \nu'$ are given by [41,42]

$$DCS^{vib}(\nu \rightarrow \nu') = \frac{4}{3} |\langle \nu' | D | \nu \rangle|^2 \frac{k'}{k} \frac{1}{q^2}, \quad (6)$$

$$\sigma_{ICS}^{vib}(\nu \rightarrow \nu') = \frac{8\pi}{3k^2} |\langle \nu' | D | \nu \rangle|^2 \log \frac{k+k'}{|k-k'|}. \quad (7)$$

Here $\langle \nu' | D | \nu \rangle$ denotes the effective transition dipole matrix element (TDM). For optically active modes this quantity can be determined from infrared absorption measurements [43]. Note that both rotational (Eqs. (3) and (4)) and vibrational (Eqs. (6) and (7)) cross-sections formulated within the Born-dipole approximation have the same angular and energy dependencies. At that time of formulation of the Born model no experimental data were available to verify its validity. Recently it was shown [44] that in non-polar molecule of CF_4 the Born-dipole approach could be used to describe both electron and positron integral cross-sections for excitation of asymmetric stretching mode. Previously [45] we noticed that this mode is so strong that it hides the Ramsauer minimum in the total cross sections. Surko et al. [44] suggested that there is a very effective charge-transfer between C and F atoms associated with asymmetric stretching. This effect results in the strong dipole transition amplitude. Consequently, the long-range coupling of transition dipole with incident electron is enough strong to make Born-approximation valid. On the other hand the short-range effects that are not described by the Born-approximation may significantly affect electron interaction with molecules characterized by much lower transition dipole moments [44]. For example, in reference [8] we showed that the near threshold vibrational cross-sections for CH_4 in the region of Ramsauer-Townsend minimum cannot be described by the Born cross-sections. The latter mode is characterized by much lower TDM [43] than the corresponding oscillations in CF_4 .

In Figure 4 we compare the Born-dipole model with the experimentally derived integral vibrational CS for the strongest optically active modes in CHF_3 and H_2O . The first molecule has the TDM comparable (though lower) with stretching mode in CF_4 , while the second molecule is characterized by very low TDM. Matrix elements were derived from IR absorption data reported by Bishop and Cheung [43]. We assumed 10% uncertainty on the latter quantity.

In more details, Figure 4a shows a comparison of swarm unfolded CS of nearly degenerate ν_{25} modes (s stretch + d stretch with the thresholds around 14 meV [46]) of CHF_3 with the sum of these two modes calculated using the Born-dipole model. Only the most recent data by Kawaguchi et al. [32] are in good agreement with Born approximation at the near threshold region. The other two considered datasets, Kushner and Zhang [30] and Bordage and Segur [31], differ in magnitudes not only with the Born-dipole but also between themselves. Moreover both authors disagree on the matter which vibrational modes contribute the most effectively to the scattering process. This clearly reflects the ambiguity of swarm analysis.

In Figure 4b we show the comparison of the Born-dipole model with cross-sections for the two fundamental modes in water recommended by Itikawa and Mason [47]. The later data were constructed taking into account both beam and swarm experiments. The Born-dipole model underestimates experimental results what could be explained

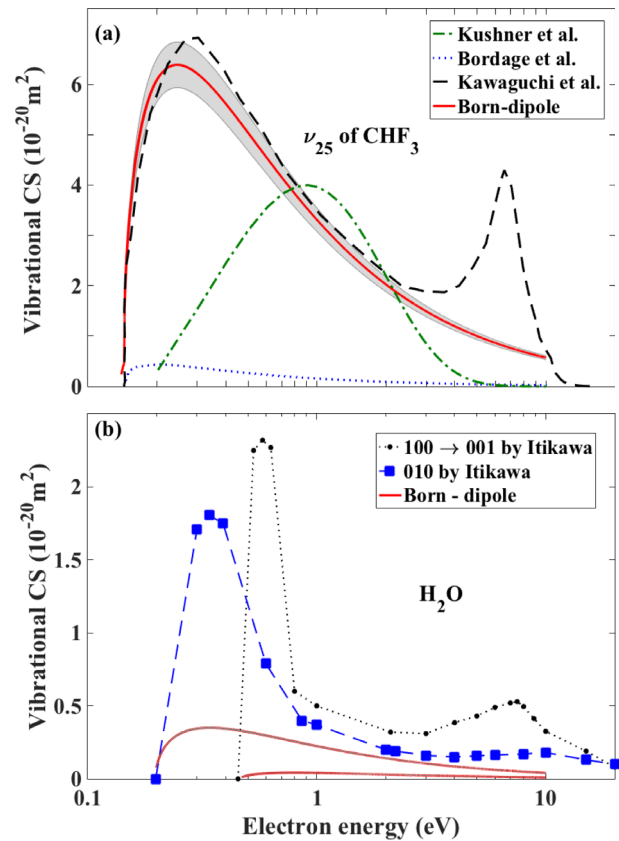


Fig. 4. Energy dependence of integral cross sections for electron impact excitation of (a) ν_{25} vibrational mode of CHF_3 and (b) $100 \rightarrow 001$ and 010 vibrational modes of H_2O . The Born-dipole model is compared with swarm-derived data by Bordage and Segur [31], Kawaguchi et al. [32], Kushner and Zhang [30] and recommended cross-sections by Itikawa and Mason [47]. The shaded areas (very small for water) represent the error bars for the Born cross-sections when 10% uncertainties are assumed on the transition dipole moments.

by the fact that TDM of H_2O is probably not strong enough to make long-range forces dominant over the short-range effects. This observation follows the hypothesis of reference [44] that strength of TDM decides about applicability of the Born-dipole model. Nevertheless a similar but broader systematic study (including more molecules) is necessary to confirm or reject this simple assumption.

5 Ionization

A simple, semiempirical method to calculate ionization cross sections for atoms have been developed by Kim and Rudd [48]. It is based on the assumption of “billiard-ball-like collision between two free electrons” [48]. In more details, this model combines a modified form of the Mott cross sections [49] (that describes the Coulomb interaction between two free electrons) with the dipole-interaction term of the plane-wave Born approximation [50] (that characterize the interaction between free and bound electrons at high collision energies). The model is known

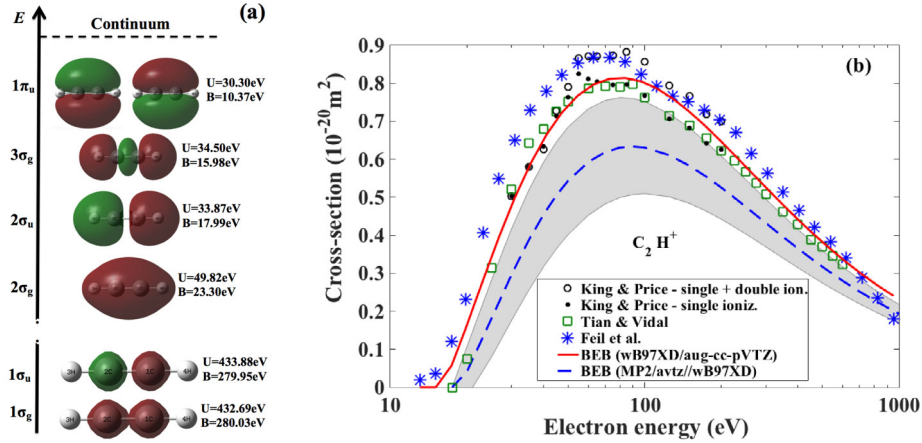


Fig. 5. (a) Molecular orbitals of C₂H₂ calculated using wB97XD/aug-cc-pVTZ basis set in the Gaussian09 code [55]. The derived binding (B) and kinetic (U) energies of electrons at each orbitals are also given. (b) Partial ionization cross-sections for the production of C₂H⁺ ion versus the energy of incident electron. The solid line represents the BEB model (wB97XD/aug-cc-pVTZ) considering only the ionization from 3 σ_g orbital in the sum of equation (8). The dashed line represents the BEB model (MP2/avtz/wB97XD) from reference [56]. The experimental data are from: King and Price [54], Tian and Vidal [58] and Feil et al. [59]. The unnormalized data of King and Price [54] were normalized to partial cross-sections for C₂H₂⁺ ion reported by Tian and Vidal [58]. The shaded area represents the error bars for BEB results [56] when 10% uncertainties are assumed on the binding and kinetic energies in equation (8).

as the binary-encounter Bethe (BEB) model. Total ionization cross section in this model, at a given collision energy E , depends solely on the binding energy of the given n th target's electron (i.e. its ionization energy B_n) and its kinetic energy U_n in the occupied orbital. It is common to normalize both E and U_n to the ionization energy: $t = E/B_n$ and $u_n = U_n/B_n$. Total ionization cross sections is then expressed by a simple formula:

$$\sigma^{ion} = \sum_n 4\pi a_0^2 \xi_n \left(\frac{R}{B_n} \right)^2 \frac{1}{t + u_n + 1} \times \left\{ 1 - \frac{1}{t} + \frac{\ln t}{2} \left(1 - \frac{1}{t^2} \right) - \frac{\ln t}{t + 1} \right\}, \quad (8)$$

where n goes through target subshells, ξ_n is the number of electrons on the n th subshell, R is the Rydberg constant and a_0 is the Bohr radius.

It was shown already by Kim and collaborators that BEB model applies to total ionization cross sections in atoms and simple molecules [51]. However, it seemed that BEB approximation [51] underestimated experimental values for molecules like CH₄, NH₃, and SO₂. We discussed in detail for CH₄ [6] that the reason for this discrepancy for molecules lies rather on the side of experimental techniques. Some old experiments measured gross total ionization cross sections from the total current of ions reaching collector. In that method, doubly charged ions (dications) were counted as two ions. Newer experiments make distinction between masses of ions, so doubly charged ions are counted correctly. However, in case of molecules, doubly charged ions are usually unstable and decay quickly into some fragments ions. Even if masses of ions are separated, the measured cross section is overestimated. Only recently, experiments [52] using a coincidence technique allow to spot two ions coming from the

same ionization event. Using such data [52] in CH₄ we were able to detract a signal from spurious counts, and show that the BEB cross section agrees with the counting total ionization cross section within 10% uncertainty that can be attributed also to experiment [53].

What is surprising is the fact that BEB applies to total ionization cross sections in a number of molecules and radicals, but it remains unknown how it is related to partial ionization cross section. Intuitively, if cross sections summed over orbitals in equation (8) agree with the experimental total ionization, one could expect that also partial cross sections can be predicted: assuming that kicking off an electron from an orbital breaks bonding, the specific fragment ions should dominate from such an event. We are not aware of such comparisons. The difficulty relies both in determining orbitals and in all possible, post-collisional dynamics of the ionized molecules, see for example [54].

Say, in CH₄ according to the valence orbital theory dating to Linus Pauling, the molecular orbitals should be formed by overlapping hybridized sp^3 carbon electrons with hydrogen electrons. But from molecular orbital theory, bonding in CH₄ comes from the unhybridized 2s and 2p orbital of carbon atoms overlapping with H electrons. This gives two distinct orbitals 1 t_2 and 2 a_1 and in consequence two ionization energies (14.1 and 27.5 eV, see [53] for details of calculation). These two values hardly correlate to experimentally observed appearance energies for fragment ions (12.6 eV for CH₄⁺ and CH₃⁺, 16.2 eV for CH₂⁺, 21.1 eV for H⁺, 22.0 eV for C⁺, 22.2 eV for CH⁺ and 22.3 eV for H₂⁺).

In C₂H₂ four molecular orbitals are involved in forming the molecule, with ionization energies 10.37 eV for 1 π_u orbital (4 electrons), 15.98 eV for 3 σ_g , 17.98 eV for 2 σ_u , and 23.30 eV for 2 σ_g orbital, see Figure 5a. These values for ionization potentials (and kinetic energies of electrons

on given orbitals) were obtained using the wB97XD/aug-cc-pVTZ orbital basis set in the Gaussian09 code, see [55].

As reviewed by King and Price [54], the experimental appearance threshold for forming single charges ions in C_2H_2 are 11.40 eV for the parent $C_2H_2^+$; for all possible fragment ions these thresholds concentrate in a narrow energy range (within 3 eV) and amount to 17.35 eV for C_2H^+ , 18.44 eV for C_2^+ , 18.83 eV or H^+ , 19.74 eV for CH_2^+ , 20.83 eV for CH^+ and 21.16 for C^+ . Note that from pure thermochemical point of view (the bond strength) the difference between C_2H^+ and C_2^+ thresholds should be as much as 5.3 eV [57] (compared to 1.1 eV from ionization experiments). Clearly, some additional energy/process lowers these thresholds. It hardly can come from molecular vibrations since the zero-point vibrational energy correction in C_2H_2 is as little as 0.7 eV.

Having in mind all limitations, in Figure 5b we show, as a simple trial attribution of BEB cross sections for ionization from a given orbital ($3\sigma_g$) to experimental partial cross sections for the production of C_2H^+ ion. Obviously, such attribution is just for sake of comparison since the agreement maybe fortuitous. More precise works, in particular for molecules with lower symmetries (i.e. with distinguishable ions from given orbitals, say CHF_2Cl , or so) would be needed. Moreover the choice of the correct basis set used in quantum mechanical calculations is also very critical since it determines the values of ionization energies (B) of outer orbitals. The latter quantities have a great effect on the BEB results. This is shown by the dashed line in Figure 5b representing another BEB calculations [56] using different molecular basis set. The latter data are given with error bars (a shaded area) that were obtained assuming 10% uncertainties on both, the ionization energy (B) and the kinetic energy of the electron (U) in the occupied orbital. This demonstrates clearly the great sensitivity of BEB on the choice of molecular basis.

In Figure 6 we perform another semi-empirical check, proposed in [53] for the series CH_4 , CH_3F , CH_2F_2 , CH_3F , and CF_4 . It was observed, that maximum of total ionization cross sections is equal, within experimental uncertainties, to $4/3$ of the average static dipole polarizability α of the molecule. In Figure 6 we extend this comparison to more molecules. We use recommended cross sections from the review by Lindsay and Mangan [60] (only F_2 has been excluded, as experiment had poor reliability) and dipole polarizabilities from CRC Handbook (for some molecules, where more than one α value is given in [18], more points with the same value of maximum ionization cross sections are presented). One see from Figure 6, that again, within experimental uncertainties the correlation: $\sigma_{\max}^{ion} = (4/3)\alpha$ holds (with σ_{\max}^{ion} in 10^{-20} m^2 and α in 10^{-30} m^3).

6 Total cross-sections

The measurements of TCS are very important because this quantity is measured in the absolute way and it serves as an indicator for amplitudes of partial processes that are essential in plasma modeling. Measurements of TCS are mainly based on the electron transmission method. In this

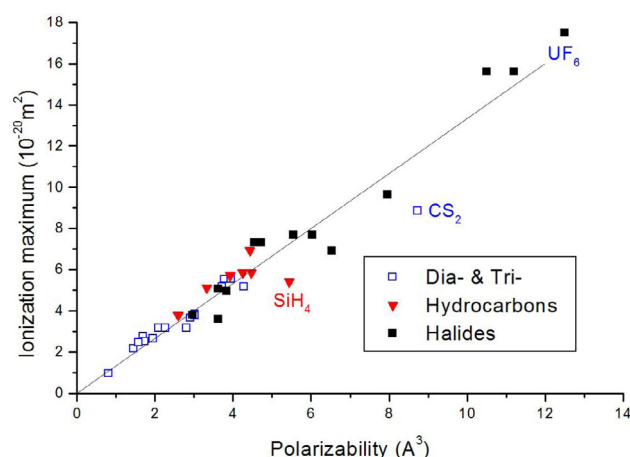


Fig. 6. Maximum of ionization cross-sections versus dipole polarizability for different molecules. The solid line is $(4/3)\alpha$. The ionization CS is taken from Landolt-Börnstein database [60], while polarizabilities are from CRC Handbook of Chemistry and Physics [18].

type of experiments the cross-sections are derived through the comparison of electron current after and before the scattering cell containing the gas under study. The main drawback of such procedure is the angular resolution error describing the inability to resolve forward scattering from the incident beam. It leads to significant underestimation of TCSs, particularly at low energies for polar molecules. To illustrate this effect in Figure 7 we compare the most recent integrated experimental DCS (shown in Fig. 1, from Refs. [16,19]) for H_2O and CH_3Cl with experimental TCS. To integrate experimental DCS, which are measured in limited angular range, we used the procedure of extrapolation to 0° and 180° described in reference [21]. This procedure includes the Born-dipole correction at low scattering angles where long-range dipolar interaction dominates. Since the elastic Born-dipole DCS (Eq. (1)) is divergent at $\theta = 0^\circ$, to avoid this singularity we use the rotational Born-dipole DCS for $0 \rightarrow 1$ transition (Eq. (3)) to approximate elastic process. Note that for a given energy, equation (3) ($0 \rightarrow 1$) is characterized by the same angular dependence as equation (1) and very similar magnitude when $k \approx k'$. Hence, assuming a very small energy loss in numerical calculations we can avoid the problem of near-zero divergence at the expense of some error around $\theta = 0^\circ$. For both considered molecules, H_2O and CH_3Cl , the inelasticity of 5 meV was assumed which is small when compared to the energies at which DCS were measured. The values of integrated cross-sections (ICS) depend on the assumed inelasticity. Assuming a larger energy loss would produce a smaller ICS; with 10 meV inelasticity, for example, the ICS would be reduced by 10% at 1 eV and by 1% at 20 eV for H_2O . To evaluate the correctness of our extrapolation and integration procedures, in Figure 7 we present also the estimated TCS obtained by summing the integrated DCS and ionization CS [60]. The agreement with experimental data at high energies (where measurements are generally reliable) is very good validating our approach.

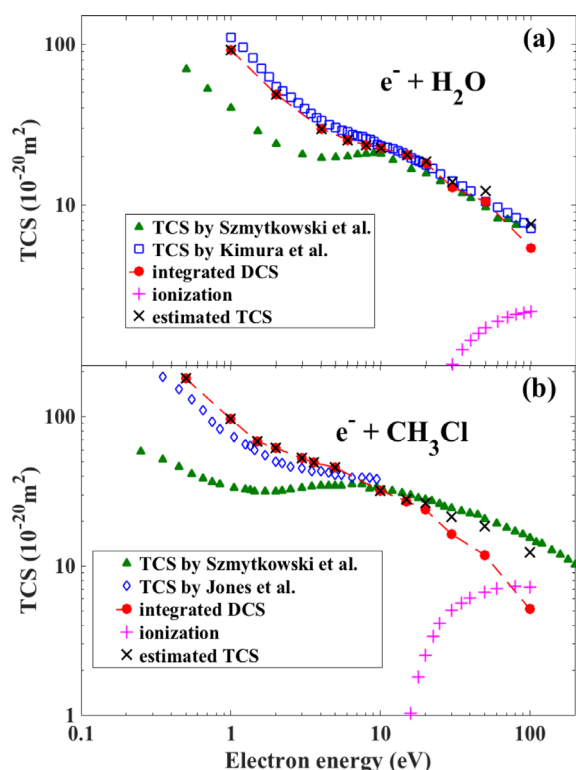


Fig. 7. Total scattering cross-sections (TCS) versus electron energy for (a) water vapour, H_2O and (b) chloromethane, CH_3Cl . The integrated experimental differential cross-sections (DCS) [16,19] including the Born-dipole corrections are compared with experimental data by Szmytkowski et al. [61,62], Kimura et al. [63] and Jones et al. [64]. The estimated TCS (\approx integrated DCS + ionization [60]) is also shown for comparison.

It is clear from Figure 7 that old measurements of Szmytkowski et al. [61,62] are probably underestimated at low energies due to the angular resolution error. The TCSs of Szmytkowski are equal to 56% and 65% of integrated DCS at 1 eV for H_2O and CH_3Cl , respectively. On the other hand TCS by Kimura et al. [63] for water and Jones et al. [64] for chloromethane are in much better agreement with integrated DCS since these authors developed procedures to correct directly measured data due to incomplete discrimination of forward scattering electrons. Many theoretical calculations [16,19,65,66] confirm the necessity of inclusion of the Born-dipole correction in processing of experimental data for polar molecules.

7 Conclusions

In the present study we analyzed briefly the applicability of the Born-dipole models for a description of elastic, rotational, vibrational and ionization cross-sections for electron collisions with polar molecules. In particular we showed that the most recent crossed-beam experiments indicate that elastic differential cross-sections (DCS) measured for many molecular targets can be potentially described by a simple Born-formula at low electron energies ($\sim E < 1$ eV) in much wider angular range than a narrow

near-zero degrees region. Of course a more quantitative study is necessary in order to estimate the Born approximation validity conditions (energy and angular ranges, magnitude of dipole moment). This requires crossed beam experiments carried out at lower energies than currently available.

The comparison of Born-dipole model with swarm-derived momentum transfer cross-sections (MTCS) for polar molecules shows that the latter varies with energy as $1/E$ for $\sim E < 1$ eV. This observation confirms the results of old studies by Christophorou et al. [4,24]. We noticed however that this conclusion is valid when we take into account MTCS containing the contribution of both elastic and rotational scattering. On the other hand when one separate both channels, the pure elastic MTCS is no longer described by the Born-formula if the rotational excitations are important.

Due to the scarcity of experimental results for rotational excitations, the Born-dipole model still remains the first choice for the estimation of corresponding cross-sections. Interestingly, the available experimental results at low impact energies are consistent with the Born model, though the more advances calculations generally disagree with this model on the magnitude of cross-sections.

Preliminary study shows that the Born-dipole model could be applicable for a description of near-threshold direct vibrational excitations of certain optically active modes characterized by sizeable transition electric dipole moments, such as stretching vibrations in CF_4 and CHF_3 . On the other hand, the Born-dipole model seems to underestimate the vibrational cross-sections for the molecules with relatively small transition strength, such as H_2O .

The Born-dipole approximation was also successfully applied for electron impact ionization of atoms and molecules within the binary encounter Bethe (BEB) model. This approach describes very well the total ionization cross-section for a large number of atoms and molecules. In this work we propose to use this model as auxiliary tool in the investigation of partial ionization cross-section for a production of specific ions. More studies are needed to evaluate the applicability of BEB for this purpose. This in turn, in combination with total and elastic cross sections can allow to delineate some partitioning schemes, like those in noble gases [67].

In addition we showed that simple linear formula describing the relation between the maximum of total ionization cross-section with the average static dipole polarizability can be applied to a broad set of different molecules, not only fluoromethanes as proved previously in reference [53].

Finally, the combination of recent experimental and theoretical results of total scattering cross-sections (TCS) for polar molecules shows that the angular resolution error in attenuation-type experiments can lead to the significant underestimation (even by a factor of few folds) of measured data at low energies. This indicates that majority of experiments carried out with polar molecules over the last half a century must be revised at low energies. Novel experimental methods have to be developed to diminish this error.

This work is supported by the Grant 2014/15/D/ST2/02358 of National Science Center in Poland. We thank Dr. Hee-Chol Choi from National Fusion Research Institute, Gunsan (Republic of Korea) for calculating electron binding and kinetic energies in C_2H_2 and Dr. T. Wróblewski from Pomeranian Academy, Słupsk (Poland) for calculating zero point vibrational energy correction.

Author contribution statement

Contributions of both authors to this work can be estimated as follows: K.F. 80% and G.K. 20%.

Open Access This is an open access article distributed under the terms of the Creative Commons Attribution License (<http://creativecommons.org/licenses/by/4.0>), which permits unrestricted use, distribution, and reproduction in any medium, provided the original work is properly cited.

References

1. R.K. Janev, *Atomic and Molecular Processes in Fusion Edge Plasmas* (Plenum, New York, 1995)
2. G. Karwasz, K. Fedus, *Fus. Sci. Technol.* **63**, 338 (2013)
3. W.J. Maciel, *Astrophysics of the Interstellar Medium* (Springer, New York, 2013)
4. L. Christophorou, J.K. Olthoff, *Fundamental Electron Interactions with Plasma Processing Gases* (Springer Science+Business Media, New York, 2004)
5. L. Sanche, *Eur. Phys. J. D* **35**, 367 (2005)
6. M.-Y. Song, J.-S. Yoon, H. Cho, Y. Itikawa, G.P. Karwasz, V. Kokoouline, Y. Nakamura, J. Tennyson, *J. Chem. Ref. Data* **44**, 023101 (2015)
7. G.P. Karwasz, A. Karbowski, Z. Idziaszek, R.S. Brusa, *Nucl. Instrum. Methods B* **266**, 471 (2008)
8. K. Fedus, G.P. Karwasz, *Eur. Phys. J. D* **68**, 93 (2014)
9. N.F. Mott, H.S.W. Massey, *The Theory of Atomic Collisions*, 3rd edn. (Clarendon Press, Oxford, 1965)
10. N.F. Lane, *Rev. Mod. Phys.* **52**, 29 (1980)
11. H. Tanaka, M.J. Brunger, M. Campbell, H. Kato, M. Hoshino, A.R.P. Rau, *Rev. Mod. Phys.* **88**, 025004 (2016)
12. H.-K. Chung, B.J. Braams, K. Bartschat, A.G. Csaszar, G.W.F. Drake, T. Kirchner, V. Kokoouline, J. Tennyson, *J. Phys. D: Appl. Phys.* **49**, 363002 (2016)
13. I. Fabrikant, *J. Phys. B* **49**, 222005 (2016)
14. S. Altshuler, *Phys. Rev.* **107**, 114 (1957)
15. M.A. Khakoo, H. Silva, J. Muse, M.C.A. Lopes, C. Winstead, V. McKoy, *Phys. Rev. A* **78**, 052710 (2008)
16. M.A. Khakoo, H. Silva, J. Muse, M.C.A. Lopes, C. Winstead, V. McKoy, *Phys. Rev. A* **87**, 049902(E) (2013)
17. S.L. Shostak, W.L. Ebenstein, J.S. Muenter, *J. Chem. Phys.* **94**, 5875 (1991)
18. D.R. Lide, *CRC Handbook of Chemistry and Physics*, 84th edn. (CRC Press, Boca Raton, FL, 2004), pp. 9–45
19. C. Navarro, A. Sakaamini, J. Cross, L.R. Hargreaves, M.A. Khakoo, K. Fedus, C. Winstead, V. McKoy, *J. Phys. B* **48**, 195202 (2015)
20. X. Shi, V.K. Chan, G.A. Gallup, P.D. Burrow, *J. Chem. Phys.* **104**, 1855 (1996)
21. K. Fedus, C. Navarro, L.R. Hargreaves, M.A. Khakoo, F.M. Silva, M.H.F. Bettge, C. Winstead, V. McKoy, *Phys. Rev. A* **90**, 032708 (2014)
22. A. Gauf, C. Navarro, G. Balch, L.R. Hargreaves, M.A. Khakoo, C. Winstead, V. McKoy, *Phys. Rev. A* **89**, 022708 (2014)
23. O.H. Crawford, *J. Chem. Phys.* **47**, 1100 (1967)
24. L.G. Christophorou, A.A. Christodoulides, *J. Phys. B* **2**, 71 (1969)
25. Y. Nakamura, *Fus. Sci. Technol.* **63**, 378 (2013)
26. M. Yousfi, M.D. Benabdessadok, *J. Appl. Phys.* **80**, 6619 (1996)
27. Hayashi's cross-section from LxCat database: <https://fr.lxcat.net>
28. J.L. Pack, R.E. Voshall, A.V. Phelps, *Phys. Rev.* **127**, 2084 (1962)
29. N.C. Jones, D. Field, S.L. Lunt, J.-P. Ziesel, *Phys. Rev. A* **78**, 042714 (2008)
30. M.J. Kushner, D. Zhang, *J. Appl. Phys.* **88**, 3231 (2000)
31. M.C. Bordage, P. Segur, *Swarm determination of electron CHF_3 collision cross sections*, ICPIG XXV, 2001, III, 253, Nagoya (Japan)
32. S. Kawaguchi, K. Satoh, H. Itoh, *Jpn. J. Appl. Phys.* **54**, 01AC01 (2015)
33. Y. Itikawa, N. Mason, *Phys. Rep.* **414**, 1 (2005)
34. Y. Itikawa, *J. Phys. Soc. Jpn* **30**, 835 (1971)
35. I. Shimamura, K. Takayanagi, *Electron-Molecule Collisions* (Plenum Press, New York, 1984), Chap. 2
36. Y. Itikawa, *J. Phys. Soc. Jpn* **32**, 217 (1972)
37. M. Rädle, G. Knoth, K. Jung, H. Ehrhardt, *J. Phys. B* **22**, 1455 (1989)
38. M. Gote, H. Ehrhardt, *J. Phys. B* **28**, 3957 (1995)
39. A. Faure, J.D. Gorfinkiel, J. Tennyson, *Mon. Not. R. Astron. Soc.* **347**, 323 (2004)
40. R. Curik, J.P. Ziesel, N.C. Jones, T.A. Field, D. Field, *Phys. Rev. Lett.* **97**, 123202 (2006)
41. K. Takayanagi, *J. Phys. Soc. Jpn* **21**, 507 (1966)
42. Y. Itikawa, *J. Phys. Soc. Jpn* **36**, 1121 (1974)
43. D.M. Bishop, L.M. Cheung, *J. Phys. Chem. Ref. Data* **11**, 119 (1982)
44. J.P. Marler, G.F. Gribakin, C.M. Surko, *Nucl. Instrum. Methods Phys. Res. B* **247**, 87 (2006)
45. G.P. Karwasz, R. Brusa, A. Zecca, *La Rivista del Nuovo Cimento* **24**, 1 (2001)
46. G.G. Raju, *Gaseous Electronics: Tables, Atoms, and Molecules* (CRC Press, New York, 2012), p. 435
47. Y. Itikawa, N. Mason, *J. Phys. Chem. Ref. Data* **34**, 1 (2005)
48. Y.-K. Kim, M.E. Rudd, *Phys. Rev. A* **50**, 3954 (1994)
49. N.F. Mott, *Proc. R. Soc. Lond. Ser. A* **126**, 259 (1930)
50. H. Bethe, *Ann. Phys.* **5**, 325 (1930)
51. Y.K. Kim, W. Hwang, N.M. Weinberger, M.A. Ali, M.E. Rudd, *J. Chem. Phys.* **106**, 1026 (1997)
52. M.D. Ward, S.J. King, S.D. Price, *J. Chem. Phys.* **134**, 024398 (2011)
53. G.P. Karwasz, P. Mozejko, M.-Y. Song, *Int. J. Mass Spectrom.* **365–366**, 232 (2014)
54. S.J. King, S.D. Price, *J. Chem. Phys.* **127**, 174307 (2007)
55. M.-Y. Song, J.-S. Yoon, H. Cho, Y. Itikawa, G.P. Karwasz, V. Kokoouline, Y. Nakamura, J. Tennyson, *J. Phys. Chem. Ref. Data*, submitted (2017)
56. Y.-K. Kim, M.A. Ali, *J. Res. Natl. Inst. Stand. Technol.* **102**, 693 (1997)

57. M. Davister, R. Loch, Chem. Phys. **189**, 805 (1994)
58. C. Tian, C. Vidal, J. Phys. B **31**, 895 (1998)
59. S. Feil, K. Gluch, A. Bacher, S. Matt-Leubner, D.K. Böhme, P. Scheier, T.D. Märk, J. Chem. Phys. **124**, 214307 (2006)
60. B.G. Lindsay, M.A. Mangan, in Landolt-Brönstein: *Numerical Data and Functional Relationships in Science and Technology – New Series/Elementary Particles, Nuclei and Atoms*; Vol. 17: *Photon and Electron Interactions with Atoms, Molecules and Ions*; Subvolume C: *Interactions of Photons and Electrons with Molecules*, edited by W. Martienssen (Springer, Berlin, Heidelberg, New York, 2003), p. 5001
61. C. Szmytkowski, Chem. Phys. Lett. **136**, 363 (1987)
62. A.M. Krzysztofowicz, C. Szmytkowski, J. Phys. B **28**, 1593 (1995)
63. M. Kimura, O. Sueoka, A. Hamada, Y. Itikawa, Adv. Chem. Phys. **111**, 537 (2000)
64. N. Jones, D. Field, J.P. Ziesel, Int. J. Mass Spectrom. **277**, 91 (2008)
65. A. Faure, J.D. Gorfinkel, J. Tennyson, J. Phys. B **37**, 801 (2004)
66. R. Zhang, A. Faure, J. Tennyson, Phys. Scr. **80**, 015301 (2009)
67. R.S. Brusa, G.P. Karwasz, A. Zecca, Z. Phys. D **38**, 279 (1996)